Am. J. Trop. Med. Hyg., 106(5), 2022, pp. 1340–1344
doi:10.4269/ajtmh.21-0416

Comparison of ^{68}Ga-DOTATOC and ^{18}F-FDG Thoracic Lymph Node and Pulmonary Lesion Uptake Using PET/CT in Postprimary Tuberculosis

Paulo Henrique Rosado-de-Castro,[1,2,3]* Thiago Pereira-de-Carvalho,[2,4] Miriam Menna Barreto,[2] Afrânio Lineu Kritski,[5] Rebecca de Oliveira Souza,[6] Sergio Altino de Almeida,[1] Valéria Cavalcanti Rolla,[7] Walter Araujo Zin,[8] Alysson Roncally Silva Carvalho,[8,9,10] and Rosana Souza Rodrigues[1,2]

[1]*Department of Internal Medicine, D'Or Institute for Research and Education, Botafogo, Rio de Janeiro, Brazil;* [2]*Department of Radiology, Federal University of Rio de Janeiro, Rio de Janeiro, Brazil;* [3]*Institute of Biomedical Sciences, Federal University of Rio de Janeiro, Rio de Janeiro, Brazil;* [4]*Department of Internal Medicine, Petropolis School of Medicine/Arthur Sá Earp Neto Faculty, Petropolis, Brazil;* [5]*Academic Tuberculosis Program, School of Medicine, Federal University of Rio de Janeiro, Rio de Janeiro, Brazil;* [6]*Department of Statistical Methods, Federal University of Rio de Janeiro, Rio de Janeiro, Brazil;* [7]*Clinical Research Laboratory on Mycobacteria, Evandro Chagas National Institute of Infectious Diseases, Fiocruz, Rio de Janeiro, Brazil;* [8]*Laboratory of Respiration Physiology, Carlos Chagas Filho Institute of Biophysics, Federal University of Rio de Janeiro, Rio de Janeiro, Brazil;* [9]*Cardiovascular R&D Centre (UnIC), Department of Surgery and Physiology, Faculty of Medicine, University of Porto, Porto, Portugal;* [10]*Laboratory of Pulmonary Engineering, Biomedical Engineering Program, Alberto Luiz Coimbra Institute of Post-Graduation and Research in Engineering, Federal University of Rio de Janeiro, Rio de Janeiro, Brazil*

Abstract. Tuberculosis (TB) remains one of the world's leading infectious cause of morbidity and mortality. Positron emission tomography (PET) associated with computed tomography (CT) allows a structural and metabolic evaluation of TB lesions, being an excellent noninvasive alternative for understanding its pathogenesis. DOTATOC labeled with gallium-68 (^{68}Ga-DOTATOC) can bind to somatostatin receptors present in activated macrophages and lymphocytes, cells with a fundamental role in TB pathogenesis. We describe ^{68}Ga-DOTATOC uptake distribution and patterns in thoracic lymph nodes (LN) and pulmonary lesions (PL) in immunocompetent patients with active postprimary TB, analyze the relative LN/PL uptake, and compare this two tracer's uptake. High uptake of both radiotracers in PL and LN was demonstrated, with higher LN/PL ratio on ^{68}Ga-DOTATOC ($P < 0.05$). Considering that LN in immunocompetent patients are poorly studied, ^{68}Ga-DOTATOC can contribute to the understanding of the complex immunopathogenesis of TB.

INTRODUCTION

Tuberculosis (TB) is the leading cause of infectious disease–related death, accounting for about 1.5 million deaths annually.[1] Postprimary tuberculosis (PPT) that occurs in immunocompetent adults differs from primary TB in terms of host susceptibility, age distribution, clinical presentation, and possible complications. PPT, caused by reinfection or dormant bacilli reactivation, accounts for 80% of all clinical cases and nearly 100% of TB transmission.[2] In immunocompetent patients, PPT affects almost exclusively the lungs and intrathoracic lymph node (LN) enlargement is rarely demonstrated in the computed tomography (CT).[2,3]

Chest X-rays and CT are useful in the morphological evaluation of TB-associated changes. Positron emission tomography (PET)/CT enables assessment of the metabolic characteristics of active PPT and primary TB.[4] Fluorine-18-labeled fluorodeoxyglucose (^{18}F-FDG) is used commonly in experimental and clinical PET/CT studies of TB, being the most validated tracer.[4] However, it lacks cellular type specificity,[4] and LN involvement in TB (especially PPT) infection is understudied.

The use of somatostatin analogs targeting surface somatostatin receptors (SSTR) not only in neuroendocrine tumors but in chronic inflammatory disease contexts has increased.[5,6] Gallium-68-labeled DOTATOC (^{68}Ga-DOTATOC) binds to receptors that can be overexpressed in activated inflammatory cells, particularly macrophages and lymphocytes,[5] which play central roles in TB infection.[7,8] The aims of this study were to describe ^{68}Ga-DOTATOC uptake distribution and patterns in thoracic LNs and pulmonary lesions (PL) in immunocompetent patients with active PPT, analyze the relative LN/PL uptake, and compare ^{68}Ga-DOTATOC and ^{18}F-FDG uptake. We hypothesize that ^{68}Ga-DOTATOC may have high PL and LN uptake, as in ^{18}F-FDG, but possible differences in uptake values may correlate to their specific targets and, thus, ^{68}Ga-DOTATOC tracer may represent a new alternative in noninvasive study of TB pathogenesis.

MATERIALS AND METHODS

Patients. Our institutional ethics committee approved this prospective observational study conducted between June of 2018 and April of 2019, and all patients provided written informed consent. Inclusion criteria were active PPT in immunocompetent adults with $<$ 30 days of TB treatment at the time of the second PET/CT acquisition. Active PPT was diagnosed by symptoms; suggestive chest X-ray findings; and *Mycobacterium tuberculosis* positivity on bacilloscopy, sputum culture, or Xpert MTB RIF. Exclusion criteria were active/recent inflammatory/tumoral disease, pregnancy/lactation, multidrug-resistant TB infection, and HIV positivity or immunosuppression. A total of 31 patients were screened by consecutive sampling, 8 agreed to participate and 1 was excluded after missing the scheduled dates for the exams.

Imaging. All patients underwent first ^{18}F-FDG PET/CT (after a $\geq$ 6 hours fast) followed by ^{68}Ga-DOTATOC PET/CT in a dedicated scanner (Siemens Biograph®; Siemens, Erlangen, Germany) at least 6 days later. Neck base–upper abdomen scans were acquired ~60 minutes after the intravenous injection of 0.12 mCi/kg ^{18}F-FDG or 0.05 mCi/kg ^{68}Ga-DOTATOC. Thoracic breath-hold CT was performed for lung parenchymal analysis. Each scan took approximately 10 minutes.

*Address correspondence to Paulo Henrique Rosado-de-Castro, Department of Radiology, Federal University of Rio de Janeiro, Avenida Carlos Chagas Filho 373, Ilha do Fundão, Rio de Janeiro, CEP: 21941-902, Brazil. E-mail: phrosado@hucff.ufrj.br

Image analysis. Two nuclear medicine specialists (SAA, PHRC) and two chest radiologists (RSR, MMB) analyzed the PET and CT images using a DICOM viewer (Osirix Imaging Software, Geneva, Switzerland). LNs with short axes $\leq$ 10 mm were deemed normal.[9] For the metabolic activity quantification from ^{18}F-FDG studies, up to three LNs and PLs each with the highest maximum standardized uptake (SUVmax) values were chosen. To compare tracer uptake, single-slice regions of interest were copied to corresponding lesions on the ^{68}Ga-DOTATOC scans (Figure 1). To minimize measurement variability,[10–12] SUVmax values were divided by an internal reference tissue (mediastinal blood pool SUVmean with a 1.0 cm^2 ROI) value, yielding $cSUVmax_{FDG}$ and $cSUVmax_{DOTATOC}$ values. To assess relative uptake, we calculated SUVmax and cSUVmax LN/PL ratios.

Statistical analysis. Statistical analysis was performed using the R application (The R Foundation for Statistical Computing, Wien, Austria). Two-way analysis of variance (ANOVA) for repeated measures were performed for SUVmax and cSUVmax using a mixed model using random intercept. The calculations used both variables on a logarithmic scale to achieve normality, which made possible the use of a parametric model. The post-hoc analysis was performed using the Tukey test. The Shapiro–Wilk test and the graphical evaluation using the qq-norm graph were used to assess the normal distribution of variables. Data are presented as medians with interquartile ranges or means with SDs, according to distribution of variables. SUVmax and cSUVmax LN/PL ratios were compared between studies using the paired samples Wilcoxon test. Spearman coefficients of correlation between LN size and SUVmax or cSUVmax measured after ^{68}Ga-DOTATOC and ^{18}F-FDG administration were determined. P values < 0.05 were deemed significant. The main analyzes were descriptive and, therefore, less dependent on the sample size.

RESULTS

Seven patients (five males, two females; mean age 29 [19–39] years) with culture-proven active PPT were included (Table 1). The TB treatment duration for ^{18}F-FDG and ^{68}Ga-DOTATOC studies were 6 (3–9; median 7) and 15 (6–17; median 7) days, respectively. Mean uptake time for ^{18}F-FDG studies was 63 minutes (range 55–68 minutes) and for ^{68}Ga-DOTATOC was 64 minutes (range 58–83 minutes). There was no statistically significant difference between uptake times ($P = 0.733$).

We analyzed and compared ^{18}F-FDG and ^{68}Ga-DOTATOC uptake in 18 PLs (mean 2.57 lesions by patient). The metabolic activity after the injection of ^{18}F-FDG was quantified and compared with the SUVmax of the same region after the injection of ^{68}Ga-DOTATOC, before and after the correction for the blood pool (Table 2). The SUVmax analysis of the mean SUVmax after injection of ^{18}F-FDG from each patient's lung lesions revealed values between 4.09 and 9.93 with a median of 7.09 (IQ = 4.46–9.72) before correction and between 3.08 and 7.50 with a median of 5.56 (IQ = 3.31–7.81) after correcting by the SUVmax of the blood pool. The SUVmax evaluation obtained from the average of the same regions after the administration of ^{68}Ga-DOTATOC resulted in values between 1.63 and 4.06 with a median of 2.09 (IQ = 0.90–3.28) before correcting and between 3.54 and 7.84 with a median of 4.36 (IQ = 3.42–5.59) after correcting by the SUVmax of the blood pool.

Likewise, LNs also had their SUVmax analyzed both in studies with ^{18}F-FDG and with ^{68}Ga-DOTATOC and tabulated before and after correction by SUVmax of the blood pool (Table 3). The median LN short-axis length was 1.0 (0.60–1.40) cm; 13 (62%) LNs were normally sized. The SUVmax analysis of the mean SUVmax from each patient's LNs after administration of ^{18}F-FDG revealed values between

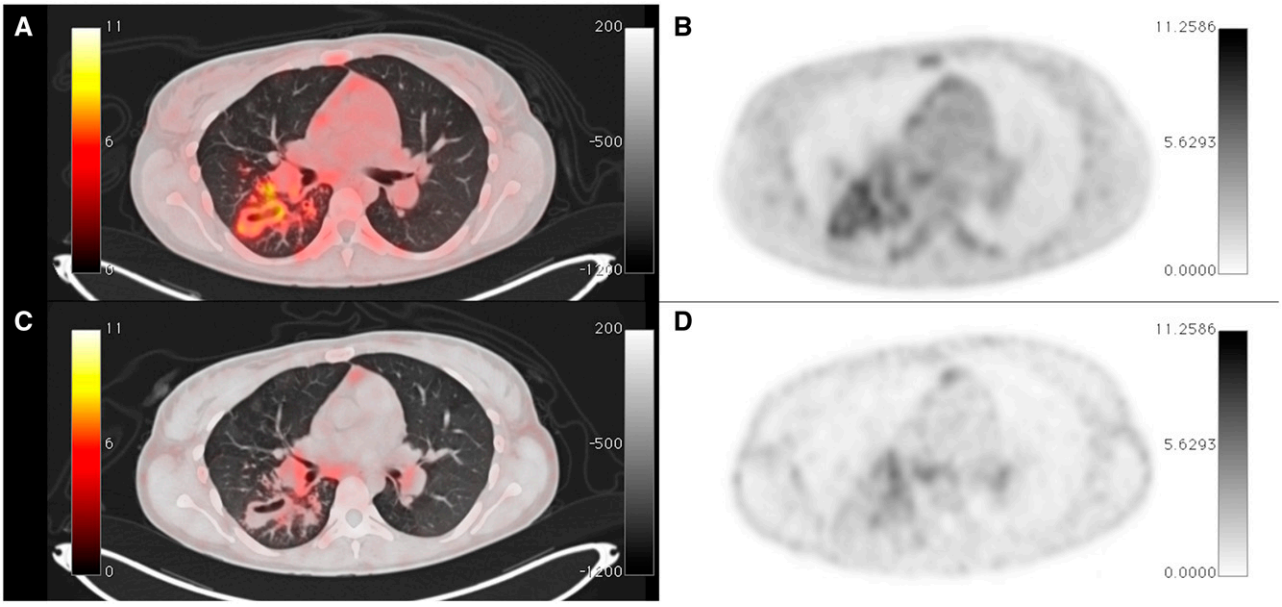

FIGURE 1. Patient 6 with active postprimary tuberculosis. Fluorine-18–labeled fluorodeoxyglucose (^{18}F-FDG) positron emission tomography/computed tomography (PET/CT) (**A** and **B**) images show remarkable uptake in pulmonary lesions and only mild in lymph nodes. However, corresponding gallium-68_labeled DOTATOC (^{68}Ga-DOTATOC) (**C** and **D**) scans reveal mild uptake in pulmonary lesions and greater relative uptake in lymph nodes, especially in subcarinal level (arrow). Vertical color bars to the left side of images (**A**) and (**C**) and color bars to the right side of images (**B**) and (**D**) in standardized uptake value. Color bar to the right side of images (**A**) and (**C**) in Hounsfield units. This figure appears in color at www.ajtmh.org.

TABLE 1
Patient characteristics and their diagnostic exams results

	Age	Sex	Interval between start of treatment and ^{18}F-FDG study (days)	Interval between studies (days)	Smear	Culture	RMT
Patient 1	24	M	3	7	+	Positive	Detectable
Patient 2	39	F	9	6	–	Positive	Detectable
Patient 3	36	M	3	7	++	Positive	Detectable
Patient 4	20	M	7	14	+	Positive	Detectable
Patient 5	24	M	3	7	++	Positive	NP
Patient 6	24	F	9	7	++	Positive	NP
Patient 7	34	M	9	17	–	Positive	Detectable

^{18}F-FDG = fluorine-18-labeled fluorodeoxyglucose; NP = not performed; RMT = rapid molecular test.

2.22 and 12.75 with a median of 3.55 (IQ = 2.01–5.09) before correction and between 1.51 and 8.55 with a median of 2.87 (IQ = 1.94–3.80) after correcting by the SUVmax of the blood pool. The SUVmax evaluation obtained from the average of the same LNs after the administration of ^{68}Ga-DOTATOC resulted in values between 1.35 and 3.00 with a median of 2.49 (IQ = 1.83–3.15) before correction and between 2.93 and 6.98 with a median of 4.40 (IQ = 3.79–5.79) after correcting by the SUVmax blood pool. There was no correlation between LN size and uptake in ^{18}F-FDG ($r = 0.2$; $P = 0.39$) or ^{68}Ga-DOTATOC ($r = -0.07$; $P = 0.76$).

We verified from the Shapiro–Wilk test that the variables logarithm of SUVmax and logarithm of cSUVmax follow a normal distribution ($P = 0.1070$, $P = 0.9380$). Such evidences are confirmed by the qq-norm graphs analysis, where quantiles of each variable are approximately aligned with the theoretical quantiles of the corresponding normal distribution. This supports the parametric analysis performed. The ANOVA tests to assess whether differences between LN and PL and the radiotracers were statistically significant for logarithm of cSUVmax ($P = 0.0231$, $P = 0.0125$) but not for logarithm of SUVmax ($P = 0.0741$, $P = 0.057$). The subgroup post-hoc analysis revealed a significant difference between LN and PL for ^{18}F-FDG ($P = 0.0416$) and between both radiotracers in LN ($P = 0.0211$). The LN/PL ratio for cSUVmax was significantly higher for ^{68}Ga-DOTATOC than for ^{18}F-FDG ($P = 0.0156$; Figure 2).

DISCUSSION

We observed the high uptake of LN, including those normally sized, and PL with both radiotracers—all LN and PL analyzed with ^{18}F-FDG had significant ^{68}Ga-DOTATOC with uptake. Few studies[13,14] with ^{68}Ga-DOTATOC in inflammatory diseases sought a direct comparison with ^{18}F-FDG, but the findings of high uptake in areas with inflammatory activity are in agreement with other studies performed in atherosclerosis and sarcoidosis.[5,6] In our study, the higher SUVmax values found in ^{68}Ga-DOTATOC compared with previous studies[6] may be related to the correction using an internal reference tissue to minimize measurement variability.[10–12,15]

In our study, LN size was not related to tracer uptake intensity and the LN/PL uptake ratio was greater for ^{68}Ga-DOTATOC than for ^{18}F-FDG. Soussan et al.[16] found LN with an average size of 15 mm, above the 10 mm found in 62% of our patients, which suggests cell activity in postprimary tuberculosis regardless of adenomegaly. ^{18}F-FDG PET/CT has revealed increased glycolytic activity in normally sized LNs in patients with latent TB, indicating that cellular activation can occur without active disease.[17] Moreover, latent TB reactivation can start in the LNs and be predicted by ^{18}F-FDG PET/CT in immunocompromised patients.[18]

SUV values from ^{68}Ga-DOTATOC have been shown to correlate with the immunohistopathological expression of SSTR, especially type 2, which is expressed on cells that play major roles in TB pathogenesis (i.e., macrophages, epithelioid cells, giant cells, and lymphocytes).[5]

Somatostatin target tissues, including lymphoid tissues, express multiple SSTR, and somatostatin analog distribution and quantification can be evaluated accurately.[5] In TB, the LNs initiate and shape adaptive immune responses, and serve as niches for *M. tuberculosis* growth and persistence.[18] In a ^{68}Ga-DOTANOC and ^{18}F-FDG PET/magnetic resonance imaging study, Naftalin et al.[6] found LN uptake in only four of eight patients with active TB, visible with both tracers. The lesion detection rate in our study was higher, with at least three LNs per patient taking up ^{68}Ga-DOTATOC, although the two tracers target similar ranges of

TABLE 2
Mean SUVmax and cSUVmax of each patient obtained from lymph nodes after administration of ^{18}F-FDG and ^{68}Ga-DOTATOC

	^{18}F-FDG		^{68}Ga-DOTATOC	
	SUVmax	cSUVmax	SUVmax	cSUVmax
Patient 1	2.42 (0.45)	1.51 (0.28)	2.08 (0.31)	3.64 (0.55)
Patient 2	12.75 (1.56)	8.55 (1.05)	1.35 (0.30)	2.93 (0.65)
Patient 3	4.50 (0.38)	3.33 (0.28)	2.83 (0.57)	5.24 (1.06)
Patient 4	4.03 (0.44)	2.62 (0.29)	2.55 (0.72)	6.23 (1.75)
Patient 5	2.22 (0.15)	3.04 (0.20)	2.66 (0.13)	4.67 (0.24)
Patient 6	3.07 (0.23)	2.96 (0.23)	2.37 (0.30)	3.88 (0.50)
Patient 7	3.70 (0.38)	2.27 (0.24)	3.00 (0.44)	6.98 (1.03)

^{18}F-FDG = fluorine-18-labeled fluorodeoxyglucose; ^{68}Ga-DOTATOC = gallium-68-labeled DOTATOC; cSUVmax = SUVmax divided by the SUVmax of the vascular pool; SUVmax = standardized maximum uptake value. Values are presented as mean (SD).

TABLE 3
Mean SUVmax and cSUVmax of each patient obtained from lung lesions after administration of ^{18}F-FDG and ^{68}Ga-DOTATOC

	^{18}F-FDG		^{68}Ga-DOTATOC	
	SUVmax	cSUVmax	SUVmax	cSUVmax
Patient 1	8.16 (0.91)	5.10 (0.57)	2.31 (0.47)	4.05 (0.82)
Patient 2	9.93 (4.83)	6.66 (3.24)	1.63 (0.57)	3.54 (1.24)
Patient 3	7.25 (1.36)	5.37 (1.00)	2.26 (0.65)	4.19 (1.20)
Patient 4	4.71 (1.97)	3.08 (1.29)	2.06 (0.59)	5.01 (1.43)
Patient 5	4.09 (0.57)	5.60 (0.78)	4.06 (0.24)	7.12 (0.42)
Patient 6	7.80 (1.02)	7.50 (0.98)	2.78 (0.70)	4.56 (1.14)
Patient 7	8.06 (5.79)	4.94 (3.55)	3.37 (3.32)	7.84 (7.72)

^{18}F-FDG = fluorine-18-labeled fluorodeoxyglucose; ^{68}Ga-DOTATOC = gallium-68-labeled DOTATOC; cSUVmax = SUVmax divided by the SUVmax of the vascular pool; SUVmax = standardized maximum uptake value. Values are presented as mean (SD).

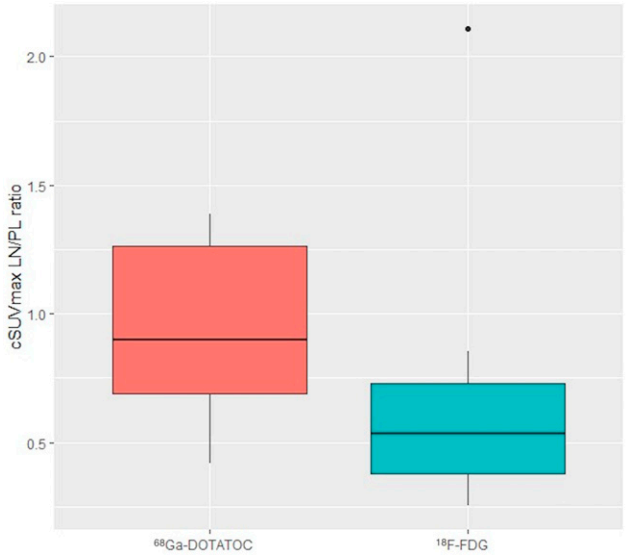

FIGURE 2. Higher mean cSUVmax (standardized maximum uptake divided by that of the mediastinal blood pool) lymph node/pulmonary lesion (LN/PL) ratio for gallium-68_labeled DOTATOC (^{68}Ga-DOTATOC) than fluorine-18–labeled fluorodeoxyglucose (^{18}F-FDG) (P = 0.0156). This figure appears in color at www.ajtmh.org.

somatostatin subtype receptors. The literature on the pathogenesis of PPT is scarcer than on latent infection and primary pulmonary TB, mainly due to the difficulty in reproducing human models in animals.[2] In addition, the information is restricted to immunological and cellular changes that occur in lung parenchyma, without assessing the repercussions on thoracic LN.[2] Thus, the greater macrophages and lymphocytes specificity of ^{68}Ga-DOTATOC[19] compared with ^{18}F-FDG,[20] and the lower ^{18}F-FDG uptake in LN and similar ^{68}Ga-DOTATOC PL uptake, led us to speculate that the high ^{18}F-FDG cSUVmax in LN represent the migration of activated defense cells without local inflammatory activity. Another factor that could, at least in part, account for the discordance in LN/PL uptake ratios (FDG versus DOTATOC) is the severe hypoxia in TB lesions, as demonstrated by Belton et al. using fluorine-18 fluoromisonidazole ([^{18}F]FMISO).[21,22]

Limitations of this study include the small sample, although our intent was to perform descriptive analysis. Additionally, performance of the PET exams on different days may have influenced comparison between the two radiotracers. However, given the slow treatment response of TB,[6] the short intervals between exams probably did not significantly affect the results.

To our knowledge, this study was the first to describe ^{68}Ga-DOTATOC uptake pattern of LN and PL in PPT and compare it with the widely validated uptake of ^{18}F-FDG. Additionally, we observed ^{18}F-FDG and ^{68}Ga-DOTATOC uptake in (even normally sized) LNs in all patients with active PPT, with higher LN/PL ratios on ^{68}Ga-DOTATOC, which raised hypothesis related to PPT parenchymal-LN cell migration despite normal LN size. No lesion had uptake restricted to one of the radiotracers and, therefore, although ^{68}Ga-DOTATOC can detect TB PL and LN, it does not add diagnostic benefit but should prompt TB as a differential diagnosis in the follow-up use of SSTR radiotracers for neuroendocrine tumors. Considering that normal-sized LN in immunocompetent patients with TB are poorly studied, ^{68}Ga-DOTATOC may contribute to in vivo TB pathogenesis studies. New studies, however, with immunocytological evaluation are needed to confirm our results and their relevance.

Received April 15, 2021. Accepted for publication February 8, 2022.

Published online April 4, 2022.

Acknowledgments: We would like to thank Carlos Chagas Filho Research Support Foundation of the State of Rio de Janeiro (FAPERJ), Brazilian National Council for Scientific and Technological Development (CNPq), André Bezerra and Adriana Moreira from TB Research Unit from Federal University of Rio de Janeiro at Caxias Health Center, and Clarissa Assumpção, Clinical Research Laboratory on Mycobacteria, Evandro Chagas National Institute of Infectious Diseases, Fiocruz for their contribution to our study.

Financial support: This work was supported by the Carlos Chagas Filho Research Support Foundation of the State of Rio de Janeiro (FAPERJ) (Grant nos. E-26/202.751/2018, E-26/202.785/2017, E-26/203.001/2018, E-26/203.279/2017, and E-26/211.867/2016) and the Brazilian National Council for Scientific and Technological Development (CNPq) (Grant nos. 302839/2017-8 and 312410/2017-4).

Authors' addresses: Paulo Henrique Rosado-de-Castro, D'Or Institute for Research and Education, Botafogo, Rio de Janeiro, Brazil, Department of Radiology, Federal University of Rio de Janeiro, Rio de Janeiro, Brazil, and Institute of Biomedical Sciences, Federal University of Rio de Janeiro, Rio de Janeiro, Brazil, E-mail: paulo.rosado@idor.org. Thiago Pereira-de-Carvalho, Department of Radiology, Federal University of Rio de Janeiro, Rio de Janeiro, Brazil, and Petrópolis School of Medicine/Arthur Sá Earp Neto Faculty, Petrópolis, Brazil, E-mail: thiago@carvalho.it. Miriam Menna Barreto, Department of Radiology, Federal University of Rio de Janeiro, Rio de Janeiro, Brazil, E-mail: miriam.menna@gmail.com. Afrânio Lineu Kritski, Academic Tuberculosis Program, School of Medicine, Federal University of Rio de Janeiro, Rio de Janeiro, Brazil, E-mail: kritskia@gmail.com. Rebecca de Oliveira Souza, Department of Statistical Methods, Federal University of Rio de Janeiro, Rio de Janeiro, Brazil, E-mail: rebecca@dme.ufrj.br. Sergio Altino de Almeida, D'Or Institute for Research and Education, Botafogo, Rio de Janeiro, Brazil, E-mail: altino.sergio@gmail.com. Valeria Cavalcanti Rolla, Clinical Research Laboratory on Mycobacteria, Evandro Chagas National Institute of Infectious Diseases, Fiocruz, Rio de Janeiro, Brazil, E-mail: valeria.rolla@ini.fiocruz.br. Walter Araujo Zin, Laboratory of Respiration Physiology, Carlos Chagas Filho Institute of Biophysics, Federal University of Rio de Janeiro, Rio de Janeiro, Brazil, E-mail: wazin@biof.ufrj.br. Alysson Roncally Silva Carvalho, Laboratory of Respiration Physiology, Carlos Chagas Filho Institute of Biophysics, Federal University of Rio de Janeiro, Rio de Janeiro, Brazil, Cardiovascular R&D Centre (UnIC), Department of Surgery and Physiology, Faculty of Medicine, University of Porto, Porto, Portugal, and Laboratory of Pulmonary Engineering, Biomedical Engineering Program, Alberto Luiz Coimbra Institute of Post-Graduation and Research in Engineering, Federal University of Rio de Janeiro, Rio de Janeiro, Brazil, E-mail: acarvalho@biof.ufrj.br. Rosana Souza Rodrigues, D'Or Institute for Research and Education, Botafogo, Rio de Janeiro, Brazil, and Department of Radiology, Federal University of Rio de Janeiro, Rio de Janeiro, Brazil, E-mail: rosana.rodrigues@idor.org.

REFERENCES

1. World Health Organization, 2016. *Global Tuberculosis Report 2016.* Geneva, Switzerland: WHO.
2. Hunter RL, 2011. Pathology of post primary tuberculosis of the lung: an illustrated critical review. *Tuberculosis (Edinb) 91:* 497–509.
3. McCullough AE, Leslie KO, 2018. Lung infections. Leslie KO, Wick MR, eds. *Practical Pulmonary Pathology: A Diagnostic Approach* (Third Edition). Elsevier, 147–226.e5. Available at: https://doi.org/10.1016/B978-0-323-44284-8.00007-7.

4. Ankrah AO, van der Werf TS, de Vries EF, Dierckx RA, Sathekge MM, Glaudemans AW, 2016. PET/CT imaging of *Mycobacterium tuberculosis* infection. *Clin Transl Imaging 4:* 131–144.
5. Anzola LK, Glaudemans AWJM, Dierckx RAJO, Martinez FA, Moreno S, Signore A, 2019. Somatostatin receptor imaging by SPECT and PET in patients with chronic inflammatory disorders: a systematic review. *Eur J Nucl Med Mol Imaging 46:* 2496–2513.
6. Naftalin CM, Leek F, Hallinan JTPD, Khor LK, Totman JJ, Wang J, Wang YT, Paton NI, 2020. Comparison of 68Ga-DOTANOC with 18F-FDG using PET/MRI imaging in patients with pulmonary tuberculosis. *Sci Rep 10:* 14236.
7. Cardona PJ, 2018. Pathogenesis of tuberculosis and other mycobacteriosis. *Enferm Infecc Microbiol Clin 36:* 38–46.
8. Lawn SD, Zumla AI, 2011. Tuberculosis. *Lancet 378:* 57–72.
9. Munden RF et al., 2018. Managing incidental findings on thoracic CT: mediastinal and cardiovascular findings. A white paper of the ACR incidental findings committee. *J Am Coll Radiol 15:* 1087–1096.
10. Azmi NHM, Suppiah S, Liong CW, Noor NM, Said SM, Hanafi MH, Kaewput C, Saad FFA, Vinjamuri S, 2018. Reliability of standardized uptake value normalized to lean body mass using the liver as a reference organ, in contrast-enhanced 18F-FDG PET/CT imaging. *Radiat Phys Chem 147:* 35–39.
11. Coura-Filho GB, Hoff AAFO, Duarte PS, Buchpiguel CA, Josefsson A, Hobbs RF, Sgouros G, Sapienza MT, 2019. 68Ga-DOTATATE PET: temporal variation of maximum standardized uptake value in normal tissues and neuroendocrine tumours. *Nucl Med Commun 40:* 920–926.
12. Duan XY, Wang W, Li M, Li Y, Guo YM, 2015. Predictive significance of standardized uptake value parameters of FDG-PET in patients with non-small cell lung carcinoma. *Braz J Med Biol Res 48:* 267–272.
13. Lee R, Kim J, Paeng JC, Byun JW, Cheon GJ, Lee DS, Chung JK, Kang KW, 2018. Measurement of ^{68}Ga-DOTATOC uptake in the thoracic aorta and its correlation with cardiovascular risk. *Nucl Med Mol Imaging 52:* 279–286.
14. Tarkin JM et al., 2017. Detection of atherosclerotic inflammation by. *J Am Coll Cardiol 69:* 1774–1791.
15. Giesel FL, Schneider F, Kratochwil C, Rath D, Moltz J, Holland-Letz T, Kauczor HU, Schwartz LH, Haberkorn U, Flechsig P, 2017. Correlation between SUVmax and CT radiomic analysis using lymph node density in PET/CT-based lymph node staging. *J Nucl Med 58:* 282–287.
16. Soussan M, Brillet PY, Mekinian A, Khafagy A, Nicolas P, Vessieres A, Brauner M, 2012. Patterns of pulmonary tuberculosis on FDG-PET/CT. *Eur J Radiol 81:* 2872–2876.
17. Ghesani N, Patrawalla A, Lardizabal A, Salgame P, Fennelly KP, 2014. Increased cellular activity in thoracic lymph nodes in early human latent tuberculosis infection. *Am J Respir Crit Care Med 189:* 748–750.
18. Ganchua SKC, White AG, Klein EC, Flynn JL, 2020. Lymph nodes-the neglected battlefield in tuberculosis. *PLoS Pathog 16:* e1008632.
19. Armani C, Catalani E, Balbarini A, Bagnoli P, Cervia D, 2007. Expression, pharmacology, and functional role of somatostatin receptor subtypes 1 and 2 in human macrophages. *J Leukoc Biol 81:* 845–855.
20. Borchert T, Beitar L, Langer LBN, Polyak A, Wester HJ, Ross TL, Hilfiker-Kleiner D, Bengel FM, Thackeray JT, 2021. Dissecting the target leukocyte subpopulations of clinically relevant inflammation radiopharmaceuticals. *J Nucl Cardiol 28:* 1636–1645.
21. More S, Marakalala MJ, Sathekge M, 2021. Tuberculosis: role of nuclear medicine and molecular imaging with potential impact of neutrophil-specific tracers. *Front Med (Lausanne) 8:* 758636.
22. Belton M et al., 2016. Hypoxia and tissue destruction in pulmonary TB. *Thorax 71:* 1145–1153.